ACS APPLIED MATERIALS & INTERFACES

www.acsami.org

Research Article

# Low Operating Voltage Carbon–Graphene Hybrid E-textile for Temperature Sensing

Gopika Rajan, Joseph J. Morgan, Conor Murphy, Elias Torres Alonso, Jessica Wade, Anna K. Ott, Saverio Russo, Helena Alves, Monica F. Craciun, and Ana I. S. Neves*

Cite This: *ACS Appl. Mater. Interfaces* 2020, 12, 29861–29867

Read Online

ACCESS | Metrics & More | Article Recommendations | Supporting Information

**ABSTRACT:** Graphene-coated polypropylene (PP) textile fibers are presented for their use as temperature sensors. These temperature sensors show a negative thermal coefficient of resistance (TCR) in a range between 30 and 45 °C with good sensitivity and reliability and can operate at voltages as low as 1 V. The analysis of the transient response of the temperature on resistance of different types of graphene produced by chemical vapor deposition (CVD) and shear exfoliation of graphite (SEG) shows that trilayer graphene (TLG) grown on copper by CVD displays better sensitivity due to the better thickness uniformity of the film and that carbon paste provides good contact for the measurements. Along with high sensitivity, TLG on PP shows not only the best response but also better transparency, mechanical stability, and washability compared to SEG. Temperature-dependent Raman analysis reveals that the temperature has no significant effect on the peak frequency of PP and expected effect on graphene in the demonstrated temperature range. The presented results demonstrate that these flexible, lightweight temperature sensors based on TLG with a negative TCR can be easily integrated in fabrics.

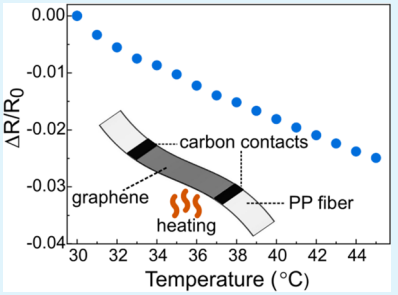


**KEYWORDS:** *e-textiles, wearables, carbon, graphene, temperature sensors, textile fibers*



## INTRODUCTION

Wearable technology is becoming a part of our lives, and the global e-textile market continues to grow at a rate of 25% according to the "Global E-textile Market 2018-2022" report.[1] With end user industries of this technology including military, sports, architecture, medical, fashion, and entertainment, one of the major drivers of this market is the high demand for health monitoring wearables. For instance, the defense sector utilizes such wearable devices to remotely monitor the health data of soldiers in order to deploy an emergency medical team and rescue personnel. These sensors would also help healthcare professionals to perform continuous monitoring of the patient's vitals.[2] Therefore, the growing implementation of health-monitoring devices subsequently increases the demand for e-textiles, textiles that have integrated electronic functionalities such as touch sensitivity, electroluminescence,[3] thermal regulation,[4] and so forth. These textile-based devices can consist of a single monofilament fiber[5] as well as woven and nonwoven fabrics.

This work focuses on temperature, being an important health parameter, fluctuations of which can cause several health-related problems. Therefore, accurate and precise measurement of the temperature is essential. Temperature sensors can be categorized into contact and noncontact sensors. Contact type sensors require physical contact with the object to be sensed using thermal conduction, while the noncontact type uses convection and radiation.[6] The commercially available contact and noncontact temperature sensors, despite giving high resolution and being highly accurate, are usually quite rigid; they feel cold and can therefore become uncomfortable for prolonged use. Several materials, such as pure metals[7] and conductive polymer composites,[8] have been demonstrated to show a large change in electrical properties with changes in the temperature. Some of the examples include metal-based resistance temperature detectors (RTDs) using platinum,[7] gold,[9] and nickel[10] in order to achieve a positive thermal coefficient of resistance (TCR).[6] However, the high processing temperature of these metals and their rigidity often make them unsuitable for heat-sensitive flexible substrates. To address this, several flexible, stretchable, biocompatible, wearable, and textile-based temperature sensors have been demonstrated over the years. These can be thermocouple sensors, thermistors, semiconductor-based sensors, flexible brain core temperature sensors, and near body ambient temperature sensors among numerous others.[11]

There have been multiple reports of temperature sensors based on printing technologies, such as silver nanoparticles on a polyethylene terephthalate (PET) substrate,[6] organic semiconductor in polycarbonate-based thermistors,[12] and thermo-

Received: May 7, 2020
Accepted: June 8, 2020
Published: June 8, 2020

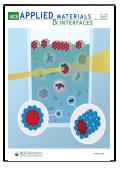







https://dx.doi.org/10.1021/acsami.0c08397
*ACS Appl. Mater. Interfaces* 2020, 12, 29861–29867

sensitive polymers on polyimide sheets,[13] and even novel approaches have also been adopted to sense the temperature such as using optical fibers.[14] However, all these techniques require subsequently attaching the flexible sensor to a fabric, or to a patch as artificial electronic skin,[15] and are therefore not completely integrated on textiles. Moreover, most of these sensors are sensitive to washing, lack mechanical stability, and would need to be patched on the skin; some also require a high supply voltage. It is therefore of great interest to develop monofilament textile temperature sensors that can be woven into the textile fabric or simply integrated into clothing at specific positions where temperature measurement is suitable in order to offer continuous temperature monitoring.

Graphene has been used for temperature sensing, with most examples relying on rigid substrates for fundamental studies.[16,17] Examples of temperature-sensing applications are mostly based on reduced graphene oxide (RGO),[18−20] which is lower in quality and purity compared to pristine graphene, and RGO composites with graphene.[21] Nonetheless, recent studies have highlighted graphene as a potential candidate for the fabrication of the next generation of e-textiles.[5,22,23]

In this study, we propose a resistive temperature sensor based on an insulating polypropylene (PP) monofilament textile fiber that uses graphene as the temperature-sensing layer and the change in resistance with temperature as the sensing parameter. Silver ink and carbon paste have been used as contacts to compare their adhesion to the textile fiber. These sensors can very easily be integrated in garments, are almost invisible because of their dimensions and optical transparency, and can operate in contact and noncontact mode. Graphene was produced by two approaches: top-down approach, chemical vapor deposition (CVD); and bottom-down approach, shear exfoliation of graphite (SEG). The proposed devices are fabricated by coating monofilament polypropylene textile fibers with graphene, as previously demonstrated by our group.[5] Along with being lightweight, eco-friendly, and recyclable, compared with other tested polymeric materials, these fibers have low thermal conductivity and high strain resistance. Furthermore, we have previously demonstrated that PP fibers can be coated with different types of graphene,[23] so their effectiveness and sensitivity to temperature has been studied in the current work. Our devices require a steady and low supply voltage of 1 V, which is suitable in terms of safety to be used in e-textile applications. These devices are particularly suited to measure the human body temperature, typically in the range of 36.5−37.5 °C, in order to avoid dangerous hypothermia (<35 °C) and hyperpyrexia (>40 °C).

## EXPERIMENTAL SECTION

**Textile Fibers.** PP fibers are tape-shaped monofilament textile fibers (0.03 mm thick and 2.4 mm wide) produced by Centexbel using an extrusion line. These fibers were rolled into a reel and cut off to the necessary length.

**Chemical Vapor Deposition of Graphene.** Trilayer graphene (TLG) was grown by chemical vapor deposition on a 0.025 mm-thick 99.999% copper foil from Alfa Aesar using a furnace by MTI systems inside a quartz tube at atmospheric pressure in an inert Ar environment. The copper foil was horizontally placed on a quartz substrate holder in the central isothermal growth zone of the reactor during the entire process. The system was evacuated and then flushed with Ar (300 sccm) to ensure the removal of any residual oxygen and moisture. The temperature is ramped up to 1000 °C (33 °C/min), and the tube is annealed at the same temperature for 30 min with a mixture of Ar (230 sccm) and $H_2$ (70 sccm). The Ar flow is stopped, and graphene growth takes place upon introduction of methane (0.1% $CH_4$ in Ar) into the tube already in the presence of hydrogen for the next 60 min. After the growth, the furnace is let to cool down to room temperature at a rate of 16 °C/min, still under a $CH_4/H_2$ flow. Single-layer graphene (SLG) was grown in a similar way but at a low pressure, ramped up at the same rate of up to 1035 °C with 100 sccm of $H_2$, grown by adding 10 sccm of $CH_4$ to the mixture for 60 s, and rapidly cooled down by opening the furnace. Few-layer graphene (FLG) grown on nickel (1 × 1 cm) was purchased from Graphene Supermarket with thickness of the film varying from one to seven layers with an average of four. All CVD-grown graphene samples were transferred as described previously,[5] but 1 M solution of $FeCl_3$ was used to chemically etch copper and nickel.

**Shear Exfoliation of Graphite.** Shear-exfoliated graphene (SEG) was produced by shear exfoliation of graphite powder (Sigma Aldrich) in deionized water and with sodium cholate as a surfactant, as previously described.[25] The suspension was left to rest overnight before the decanting step to remove the unexfoliated excess graphite. PP fibers were coated with graphene films produced from these suspensions using the IDT (isopropyl alcohol-assisted direct transfer) method also described previously but at a temperature of 85 °C. It should be noted that these SEG-coated PP fibers differ from the SEG-coated fibers demonstrated previously,[3] which were transferred via a cellulose-based dip-coating method. It was found that these films contain an average of three layers.[25]

**Raman Spectroscopy.** A WITec Alpha 300R (confocal Raman system) spectrometer (WITec Inc., ULM, Germany) equipped with a thermoelectrically cooled CCD detector (−60 °C) was used with a 532 nm laser excitation source backscattered light collection with a 50× Zeiss objective (EC EPIPLAN NA 0.7) and a spot size of 388 nm. The spectrometer grating of 600 or 1800 g/mm was used. The analysis software used was WITec Project Plus. Temperature-dependent Raman spectra were recorded at a heating rate of 5 °C/min, and measurements were taken every 5 °C using the Renishaw Raman system. We used a long working-distance 50× objective and 514 nm argon ion laser at 10−50% power in nitrogen to avoid sample damage.

**Temperature-Dependent Electrical Resistance Measurements.** The electric conductivity of the sensors was measured by a two-probe method using tungsten probes and a Keithley 2400 source measure unit. Carbon paste and silver ink were used to draw the contacts to facilitate the measurements. The fibers coated with contacts were immobilized on a rigid substrate (glass slide), then the probes were placed on the contacts. A hot plate (Thermo Scientific, Super Nuova) was used to increase the temperature at an incremental step of 1 °C. To obtain the change in resistance, the temperature was increased from 30 to 70 °C. The probes are placed at a set channel length of 1 cm (channel width is the width of the fiber, 2.4 mm) to make the measurements at different temperatures comparable, and the current was recorded with an imposed voltage of 1 V.

**Optical Transmittance Measurements.** TLG was transferred to glass to acquire the transmission spectra using a custom-built UV−vis microspectrometer. Light from an incandescent bulb was focused onto the samples through a condenser lens, collected by a 20× microscope objective, then delivered to the entrance slit of a spectrometer (Princeton Instruments Acton SP2500) equipped with a 1800 g/mm and CCD camera (Princeton Instruments PIXIS400).[26] Transmittance as a function of wavelength was calculated as $T = I/I_0$ where $I$ is the measured spectral intensity through the sample, and $I_0$ is the incident light intensity. Corrections to account for the optics and gratings efficiencies at different wavelengths were applied using the Princeton Instruments IntelliCal system.[26]

**Bending Tests.** In order to investigate the flexibility and mechanical resilience of the PP conductive fibers, graphene-coated fibers were subjected to a series of bending tests of up to 1000 bending cycles with a fixed bending radius of 5 mm, and the effect of bending on their electrical resistance, back to a flat position after bending, and temperature sensitivity was studied.

**Washing Tests.** Washability of the temperature sensors were studied by washing the graphene-coated fibers in a solution of


https://dx.doi.org/10.1021/acsami.0c08397
ACS Appl. Mater. Interfaces 2020, 12, 29861−29867

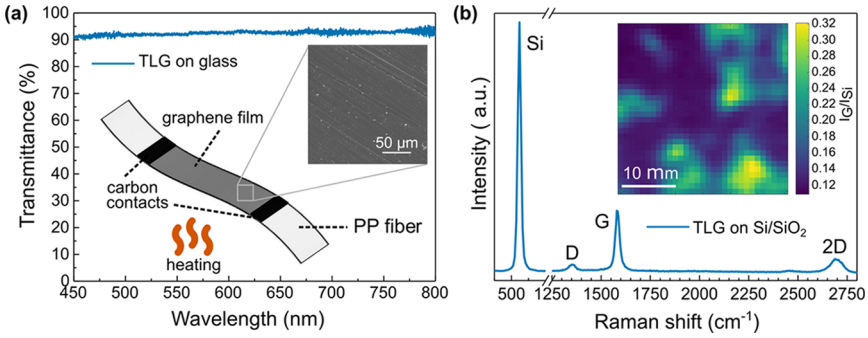


**Figure 1.** (a) Transmittance as a function of wavelength for TLG on glass with an SEM image of graphene-coated fibers (SEM study in the Supporting Information) and depiction of the temperature sensor with graphene-coated PP fibers and carbon contacts in the inset. (b) Raman spectrum of TLG on $Si/SiO_2$, highlighting the characteristic graphene Raman peaks with a 30 × 30 $\mu$m in the inset of $I_G/I_{Si}$ showing how the layers are distributed (three layers correspond to 0.28 $I_G/I_{Si}$).

commercial laundry detergent and tap water for 60 min using a glass beaker and a magnetic stirring bar. Several parameters such as the temperature (30, 40, and 50 °C), spin speed (400, 800, and 1000 rpm), and laundry detergents (regular and for sensitive fabrics) were varied. This was done to emulate the use of a washing machine. Initial resistance prior to washing and final resistance after washing were recorded.

**Scanning Electron Microscopy.** A TESCAN VEGA3 scanning electron microscope (SEM) was used to perform morphological characterization of the sensor's surface at an accelerating voltage of 10 kV and working distance of 10 mm.

## RESULTS AND DISCUSSION

The textile temperature sensor architecture is depicted in the Figure 1a inset and consists of (1) graphene as the temperature-sensing layer, (2) PP textile fiber as the flexible substrate, and (3) carbon paste as the contact material. Different types of graphene coatings have been employed. The three types of graphene grown by CVD are as follows: single-layer graphene (SLG), purposely developed trilayer graphene (TLG) grown on copper, and few-layer graphene (FLG) grown on nickel. Additionally, graphene films produced by shear exfoliation of graphite were also tested. In addition to carbon paste, silver ink was also tested as a contact material but with poor results due to the general lack of flexibility of metallic contacts. The different graphene films were obtained and transferred onto the PP fibers as described in the previous section.

Optical transmittance analysis was performed to ascertain the number of layers of graphene (Figure 1a). For this purpose, TLG was transferred to glass. Numerical and experimental studies have found that the optical transmittance of graphene follows a nonlinear negative exponential function of the form $T = (1 + 1.13\pi\alpha N/2) - 2$, which gives a good description of the transmittance of light through multilayer graphene in the visible range.[27] Here, $N$ is the number of graphene layers; $\alpha = e\hbar 2/c \approx 1/137$, which is the fine structure constant; and 1.13 is the estimation of the correction coefficient. The experimental data for optical transmittance in TLG was extracted at 550 nm since at this wavelength it is independent of the stacking sequence. It was found to be ca. 91.6%, which corresponds to a calculated number of layers of three (Figure S1, Supporting Information). Figure 1b shows the characteristic Raman spectrum of TLG on $Si/SiO_2$ with the most notable features of the spectrum being the Si peak at 520.7 $cm^{-1}$ and the distinctive graphene peaks: the disorder-induced D peak at 1351 $cm^{-1}$, G peak corresponding to the $E_{2g}$ mode at 1592 $cm^{-1}$, and the overtone of the D band as the 2D peak at 2680 $cm^{-1}$.[28] Following the method developed by Koh et al.,[29] which consists of comparing the intensity of the G peak of the graphene film transferred onto $Si/SiO_2$ and the first-order optical phonon peak of Si, $I_G/I_{Si}$, the number of graphene layers on the same TLG films transferred onto $Si/SiO_2$ was found to be three, corresponding to an $I_G/I_{Si}$ ratio of ca. 0.28. This method was employed to an area of 30 × 30 $\mu m^2$ of the produced TLG film (inset of Figure 1b with details in Figure S2, Supporting Information), showing that the sample is homogeneously dispersed in terms of number of layers, ranging from one to four layers, with trilayer being the predominant. Raman spectroscopy was also used to identify the presence of graphene on PP after transfer. The Raman spectra for SLG-, TLG-, FLG-, and SEG-coated PP, as well as for the bare PP fiber, are shown in Figure S3 (Supporting Information). In these, the G peak appears in a relatively unpopulated area of the spectrum and, although small, is therefore clearly identifiable, whereas the 2D peak partially overlaps a peak from the PP fiber. A more detailed characterization of the purposely developed TLG films can be found in the Supporting Information. These results are in agreement with the optical transmittance tests.

To determine the temperature-sensing properties of graphene-coated PP fibers, the devices were electrically characterized, and the variation of resistance was measured with an externally controlled temperature from 30 to 70 °C in the contact mode. Figure S4 (Supporting Information) shows the temperature dependence of the resistance of PP fibers coated with the different types of graphene measured with carbon contacts. No trend in the change of resistance has been observed in the PP fiber coated with FLG, suggesting that this type of graphene is not a good candidate for temperature sensing perhaps due to the larger number of layers. SEG on PP shows some sensitivity to temperature while using both carbon and silver paste as contacts, as shown in Figure S5 (Supporting Information). However, it was observed that this is not repeatable, with one layer only not being robust enough for the purpose. Although SEG has fewer layers than FLG, the nature of top-down graphene is different, with these films consisting of overlapping flakes rather than merging crystalline domains. Furthermore, since the SEG process requires the use of a surfactant, sodium cholate, the presence of its residues on the film might also contribute to these results, as demonstrated previously in ref 24 with a detailed study. Figure 2a shows that in the case of TLG-coated fibers, the resistance decreases with


https://dx.doi.org/10.1021/acsami.0c08397
ACS Appl. Mater. Interfaces 2020, 12, 29861−29867

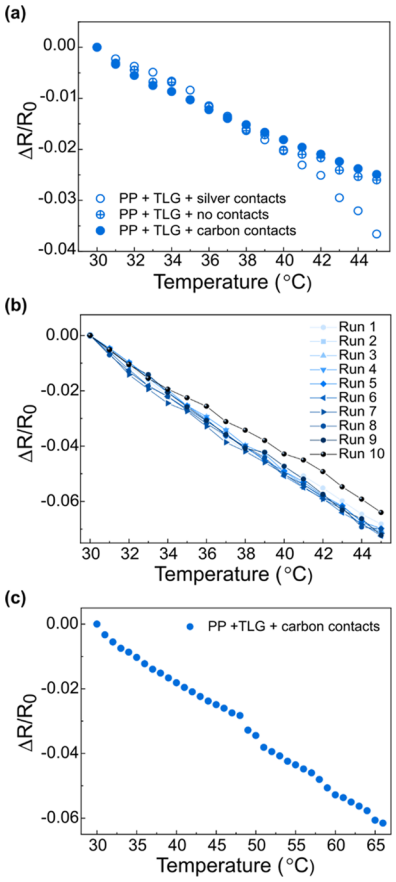


**Figure 2.** Sensitivity as a function of temperature for a TLG sensor in contact mode (a) in the human body temperature range with different types of contacts, (b) for multiple body temperature cycles, and (c) for a larger temperature range of 30−70 °C.

the increase in the temperature, the negative temperature coefficient (NTC) behavior showing linearity between ca. 30 and 45 °C. The errors associated with these measurements are considerably small, as shown in Figure S6 (Supporting Information). We defined the sensitivity of our sensors as the ratio of the change in resistance to the initial resistance ($\Delta R/R_0$). The thermal coefficient of resistance can be defined by TCR = $R_b - R_a/R_a(\Delta T)$, where $\Delta T = T_b - T_a$ is the change in the temperature, and $R_a$ and $R_b$ are the initial and final resistance, respectively. The calculated TCR for TLG-coated fibers is ∼−0.0017 °C$^{-1}$, which is similar to, albeit slightly higher than, other reported values for graphene.[30−32] A similar behavior has been reported for graphene-based thermistors on a PDMS substrate, printed graphene electrodes on a PET substrate,[33] and multiwall carbon nanotubes.[34] It has also been shown that for graphene, which is a semimetal,[35] quenching of electrical resistance takes place when the temperature exceeds room temperature.[36] Figure 2a also shows that the linear behavior is observed with and without the carbon paste contacts but is suppressed when the silver paste is used as contacts instead, making these contacts unsuitable for the purpose of temperature sensing. It should be noted that the supply voltage for all these devices was 1 V, suggesting low operating voltage applications. In fact, the linear response can also be observed at 0.5 V (Figure S7, Supporting Information) but with a larger sensing error. In terms of robustness, Figure 2b shows that the sensing behavior remains mostly unchanged over 10 temperature cycles with good linearity (see the Supporting Information for details). Above ca. 48 °C, the resistance deviates from linearity as can be seen in Figure 2c. Power consumption for these sensors were found to be in the range of 12−14 $\mu$W, suggesting that these devices are easily applicable in low-power electronics. A more detailed characterization of the sensing behavior with different contact materials, silver and just the tungsten probes, is shown in Figures S8 and S9 in the Supporting Information. Once again, silver ink did not show the same behavior, and we believe that this is related with poor adhesion of silver ink to the graphene film compared to carbon paste. With just the tungsten probes in direct contact with graphene, the response was still linear. Finally, in order to demonstrate the ability of these TLG-based sensors to continuously monitor the ambient temperature in the noncontact sensing mode (sensing the air rather than the surface they are in contact with), they were measured against a commercial temperature sensor with time as the independent variable and using a hot air gun. As shown in Figure S10 (Supporting Information), the TLG sensor follows a similar trend as the commercial sensor.

The graphene-coated PP fibers were subjected to scanning electron microscopy analysis to obtain information about the surface topology after exposure to temperature. It can be seen (Figure S11, Supporting Information) that for uncoated PP fibers and for PP fibers coated with all types of graphene coating employed, there are no visible changes in the topography after temperature cycling. The CVD graphene coatings are very thin, so the extrusion lines of the PP fibers are visible particularly with TLG and slightly blurred with the thicker FLG.[5,24] However, SEG-coated samples displayed cracks in the coating to begin with (Figure S12, Supporting Information). Unlike the continuous CVD films, SEG films comprise overlapping graphene flakes, possibly considerably thick in places, and this might explain why these films were so unreliable for the purpose of temperature sensing.

Temperature-dependent Raman studies were performed to further understand if temperature exposure affects the PP and TLG within the range of room temperature to 85 °C. To study this, five distinct peaks in Raman spectra of PP were chosen: peak A at 841 cm$^{-1}$, peak B at 998 cm$^{-1}$, peak C at 1151 cm$^{-1}$, peak D at 1328 cm$^{-1}$, and peak E at 1460 cm$^{-1}$. It can be seen in Figure S13 (Supporting Information) that the Raman spectra of PP do not show any significant change in the 25−85 °C temperature range. Figure 3 shows the fitted G peak position of TLG on PP as a function of temperature in the range of 25−85 °C. Following the work of Calizo et al.,[37] we fitted our data with a straight line. A calculated slope of

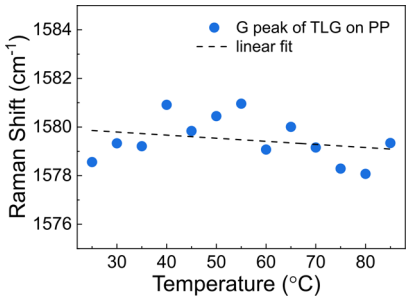


**Figure 3.** Raman shift of the G peak of TLG on PP as a function of temperature. The data fits a straight line with a slope of −0.01273, similar to the value obtained by Calizo et al.[37]


https://dx.doi.org/10.1021/acsami.0c08397
ACS Appl. Mater. Interfaces 2020, 12, 29861−29867

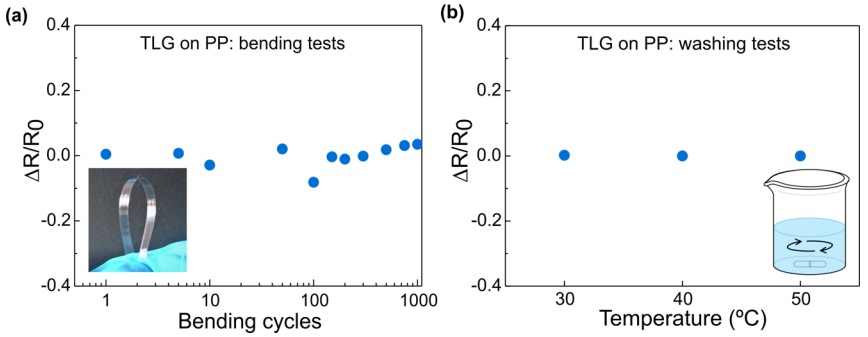


**Figure 4.** Sensitivity of a TLG-coated device as a function of (a) 5 mm-radius bending cycles with an inset of a photo of a bent PP fiber and (b) different temperatures for 60 min at 1000 rpm washing tests with an inset of an illustration of the test.

$-0.0127$ $cm^{-1}/°C$ is comparable to a slope of $-0.015$ $cm^{-1}/°C$ for bilayer graphene that was observed by Calizo et al.[37] The slope is evident of the behavior that there is a decrease in the G peak position as a function of temperature as expected. As the Raman data shows, there are no structural changes or any negative effects of the temperature on the PP and TLG and that TLG is indeed showing the expected temperature dependence.

The mechanical stability (Figure 4a) and washability (Figure 4b) tests show that there is no significant change in resistance of CVD graphene with multiple washing and bending, which is in agreement with previous studies.[3,5,24] The changes observed with bending could be minimized by locating these textile temperature sensors in the torso area below or near the armpit, for example, a place where temperature is usually taken with conventional thermometers and where minimizing the strain is applied from lifting the arms, for example. The same bending study was performed with SEG with a much higher change in resistance (Figure S14, Supporting Information). Although it was observed that the SEG is resistant to bending stress initially, its devices are affected by it after several bending cycles. This might be because of the graphene flakes detaching and/or being displaced from the PP fiber surface during rigorous washing and bending. It was observed that CVD graphene performs better than SEG when different parameters such as washing temperature, washing spin speed, and laundry detergents were varied, and the change in resistance was recorded (detailed plots in Figure S14, Supporting Information). This was done to emulate the washing machine use. Nevertheless, a temperature sensor for human body temperature monitoring would require encapsulation in order to prevent direct contact of graphene with the skin and environment, which would also protect the sensing layer from abrasion. It should be noted that this additional encapsulation layer would be placed on the outside of the sensor and is therefore not expected to interfere with the temperature sensing. An appropriate choice of an encapsulating polymer and thickness of the encapsulating layer would ensure the mechanical properties of the device would not change significantly.

## CONCLUSIONS

Graphene-based textiles for temperature sensing were fabricated and characterized. It was found that trilayer graphene on production by the chemical vapor deposition process along with carbon paste contacts produced a consistent temperature sensing from 30 to 45 °C, operation of which requires a low input voltage, making it suitable for low power wearable technology. Durability, flexibility, transparency, and washability of the devices were studied. It has also been demonstrated that despite the scalability of graphene inks, graphene grown by chemical vapor deposition is more suitable for temperature sensors. The effect of temperature on the Raman spectrum of the trilayer graphene-coated textile fiber was studied, and redshift was observed in the G mode of graphene, while the studied peaks of the polypropylene substrate showed no significant change in the examined temperature range. These sensors have a potential application in continuous measurement of the human body temperature while being integrated in garments or of the ambient temperature while being integrated in upholstery.

## ASSOCIATED CONTENT

### Supporting Information

The Supporting Information is available free of charge at https://pubs.acs.org/doi/10.1021/acsami.0c08397.

Detailed characterization of the different devices and material combinations described (transmittance, Raman, SEM); sensitivity of devices with different coatings, contacts, and number of cycles; sensitivity of devices at a lower voltage; and bending and washability tests (PDF)

## AUTHOR INFORMATION

### Corresponding Author

**Ana I. S. Neves** − *College of Engineering, Mathematics and Physical Sciences, University of Exeter, EX4 4QF Exeter, United Kingdom;* orcid.org/0000-0002-4581-525X; Email: a.neves@exeter.ac.uk

### Authors

**Gopika Rajan** − *College of Engineering, Mathematics and Physical Sciences, University of Exeter, EX4 4QF Exeter, United Kingdom*

**Joseph J. Morgan** − *College of Engineering, Mathematics and Physical Sciences, University of Exeter, EX4 4QF Exeter, United Kingdom*

**Conor Murphy** − *College of Engineering, Mathematics and Physical Sciences, University of Exeter, EX4 4QF Exeter, United Kingdom*

**Elias Torres Alonso** − *College of Engineering, Mathematics and Physical Sciences, University of Exeter, EX4 4QF Exeter, United Kingdom*

**Jessica Wade** − *Department of Physics and Centre for Plastic Electronics, Imperial College London, London SW7 2AZ, United Kingdom;* orcid.org/0000-0003-2866-3941



https://dx.doi.org/10.1021/acsami.0c08397
ACS Appl. Mater. Interfaces 2020, 12, 29861−29867

**Anna K. Ott** − *College of Engineering, Mathematics and Physical Sciences, University of Exeter, EX4 4QF Exeter, United Kingdom*

**Saverio Russo** − *College of Engineering, Mathematics and Physical Sciences, University of Exeter, EX4 4QF Exeter, United Kingdom*

**Helena Alves** − *Department of Physics and CICECO, University of Aveiro, 3819-130 Aveiro, Portugal; Department of Physics, Instituto Superior Tecnico, University of Lisbon, 1040-001 Lisbon, Portugal;* orcid.org/0000-0002-2971-9241

**Monica F. Craciun** − *College of Engineering, Mathematics and Physical Sciences, University of Exeter, EX4 4QF Exeter, United Kingdom*

Complete contact information is available at: https://pubs.acs.org/10.1021/acsami.0c08397

### Author Contributions

The manuscript was written through contributions of all authors. All authors have given approval to the final version of the manuscript.

### Notes

The authors declare no competing financial interest.

## ■ ACKNOWLEDGMENTS

The authors acknowledge financial support from the European Commission for project "E-TEX", H2020-MSCA-IF-2015-704963, EPSRC grant EP/S019855/1 and EP/M001024/1; the College of Engineering Mathematics and Physical Sciences, University of Exeter for the PhD studentship; and the Portuguese Foundation for Science and Technology grants IF/01088/2014, UIDB/50011/2020, and POCI-01-0145-FEDER-032072. G.R. and A.N. would like to thank Mr. Fred Rose for the sensor sketch and Ms. Catherine Edington and Ms. Saskia Sherwood for the assistance with washing tests. We would like to thank Dr. Peter Armitage for producing the measuring setup for the electrical conductivity measurements, Dr. Ellen M. Green for the help with the Raman mapping, Dr. Isabel de Schrijver for providing the PP fibers, Mr. Mark Heath for his assistance in the clean room, and Dr. Hong Chang for the assistance with SEM imaging. We would like to express our gratitude to Prof Ji-Seon Kim for the use of the temperature-dependent Raman system.

## ■ REFERENCES

(1) Technavio 2018 Global E-textile Market 2018-2022 SKU: IRTNTR20241.

(2) Catarino, A. P.; Carvalho, H.; Dias, M. J.; Pereira, T.; Postolache, O.; Girão, P. S. Continuous Health Monitoring Using E-Textile Integrated Biosensors. *International Conference and Exposition on Electrical and Power Engineering 2012*, IEEE, 2012, 605.

(3) Torres Alonso, E.; Rodrigues, D. P.; Khetani, M.; Shin, D.-W.; De Sanctis, A.; Joulie, H.; de Schrijver, I.; Alves, H.; Neves, A. I. S.; Russo, S.; Craciun, M. F. Graphene Electronic Fibres With Touch-Sensing and Light-Emitting Functionalities For Smart Textiles. *npj Flexible Electron.* **2018**, *2*, 25.

(4) Gao, T.; Yang, Z.; Chen, C.; Li, Y.; Fu, K.; Dai, J.; Hitz, E. M.; Xie, H.; Liu, B.; Song, J.; Yang, B.; Hu, L. Three-Dimensional Printed Thermal Regulation Textiles. *ACS Nano* **2017**, *11*, 11513−11520.

(5) Neves, A. I. S.; Bointon, T. H.; Melo, L. V.; Russo, S.; de Schrijver, I.; Craciun, M. F.; Alves, H. Transparent Conductive Graphene Textile Fibers. *Sci. Rep.* **2015**, *5*, 9866.

(6) Ali, S.; Hassan, A.; Bae, J.; Lee, C. H.; Kim, J. All-Printed Differential Temperature Sensor for the Compensation of Bending Effects. *Langmuir* **2016**, *32*, 11432−11439.

(7) Moser, Y.; Gijs, M. A. M. Miniaturized Flexible Temperature Sensor. *J. Microelectromech. Syst.* **2007**, *16*, 1349−1354.

(8) Király, A.; Ronkay, F. Temperature Dependence of Electrical Properties in Conductive Polymer Composites. *Polym. Test.* **2015**, *43*, 154−162.

(9) Ahn, C. H.; Park, H. W.; Kim, H. H.; Park, S. H.; Son, C.; Kim, M. C.; Lee, J. H.; Go, J. S. Direct Fabrication of Thin Film Gold Resistance Temperature Detection Sensors on a Curved Surface Using a Flexible Dry Film Photoresist and Their Calibration up to 450 °C. *J. Micromech. Microeng.* **2013**, *23*, No. 065031.

(10) Santos, E. J. P.; Vasconcelos, I. B. RTD-Based Smart Temperature Sensor: Process Development and Circuit Design *IEEE 26th International Conference on Microelectronics*; IEEE, 2008, 333.

(11) Samal, R.; Roult, C. S. Wearable and Flexible Sensors Based on 2D and Nanomaterials. In *Fundamentals and Sensing Applications of 2D Materials*, Woodhead Publishing Elsevier, 2019; p 437−463.

(12) Lebedev, V.; Laukhina, E.; Laukhin, V.; Somov, A.; Baranov, A. M.; Rovira, C.; Veciana, J. Investigation of Sensing Capabilities of Organic Bi-Layer Thermistor in Wearable E-Textile and Wireless Sensing. *Org. Electron.* **2017**, *42*, 146−152.

(13) Bielska, S.; Sibinski, M.; Lukasik, A. Polymer Temperature Sensor for Textronic Applications. *Mater. Sci. Eng., B* **2009**, *165*, 50−52.

(14) Li, H.; Yang, H.; Li, E.; Liu, Z.; Wei, K. Wearable Sensors in Intelligent Clothing for Measuring Human Body Temperature Based on Optical Fiber Bragg Grating. *Opt. Express* **2012**, *20*, 11740−11752.

(15) Jo, H. S.; An, S.; Kwon, H.-J.; Yarin, A. L.; Yoon, S. S. Transparent Body-Attachable Multifunctional Pressure, Thermal, and Proximity Sensor and Heater. *Sci. Rep.* **2020**, *10*, 2701.

(16) Davaji, B.; Cho, H. D.; Malakoutian, M.; Lee, J.-K.; Panin, G.; Kang, T. W.; Lee, C. H. A Patterned Single Layer Graphene Resistance Temperature Sensor. *Sci. Rep.* **2017**, *7*, 8811.

(17) Sun, P.; Zhu, M.; Wang, K.; Zhong, M.; Wei, J.; Wu, D.; Zhu, H. Small Temperature Coefficient of Resistivity of Graphene/Graphene Oxide Hybrid Membranes. *ACS Appl. Mater. Interfaces* **2013**, *5*, 9563−9571.

(18) Liu, G.; Tan, Q.; Kou, H.; Zhang, L.; Wang, J.; Lv, W.; Dong, H.; Xiong, J. A Flexible Temperature Sensor Based on Reduced Graphene Oxide for Robot Skin Used in Internet of Things. *Sensors* **2018**, *18*, 1400.

(19) Abid; Sehrawat, P.; Islam, S. S.; Mishra, P.; Ahmad, S. Reduced Graphene Oxide (rGO) Based Wideband Optical Sensor and the Role of Temperature, Defect States and Quantum Efficiency. *Sci. Rep.* **2018**, *8*, 3537.

(20) Trung, T. Q.; Le, H. S.; Dang, T. M. L.; Ju, S.; Park, S. Y.; Lee, N.-E. Freestanding, Fiber-Based, Wearable Temperature Sensor with Tunable Thermal Index for Healthcare Monitoring. *Adv. Healthcare Mater.* **2018**, *7*, 1800074.

(21) Wang, Z.; Gao, W.; Zhang, Q.; Zheng, K.; Xu, J.; Xu, W.; Shang, E.; Jiang, J.; Zhang, J.; Liu, Y. 3D-Printed Graphene/Polydimethylsiloxane Composites for Stretchable and Strain-Insensitive Temperature Sensors. *ACS Appl. Mater. Interfaces* **2019**, *11*, 1344−1352.

(22) Karim, N.; Afroj, S.; Malandraki, A.; Butterworth, S.; Beach, C.; Rigout, M.; Novoselov, K. S.; Casson, A. J.; Yeates, S. G. All Inkjet-Printed Graphene-Based Conductive Patterns for Wearable E-Textile Applications. *J. Mater. Chem. C* **2017**, *5*, 11640−11648.

(23) Karim, N.; Afroj, S.; Tan, S.; He, P.; Fernando, A.; Carr, C.; Novoselov, K. S. Scalable Production of Graphene-Based Wearable E-Textiles. *ACS Nano* **2017**, *11*, 12266−12275.

(24) Neves, A. I. S.; Rodrigues, D. P.; De Sanctis, A.; Alonso, E. T.; Pereira, M. S.; Amaral, V. S.; Melo, L. V.; Russo, S.; de Schrijver, I.; Alves, H.; Craciun, M. F. Towards Conductive Textiles: Coating Polymeric Fibres With Graphene. *Sci. Rep.* **2017**, *7*, 4250.

(25) Shin, D.-W.; Barnes, M. D.; Walsh, K.; Dimov, D.; Tian, P.; Neves, A. I. S.; Wright, C. D.; Yu, S. M.; Yoo, J.-B.; Russo, S.; Craciun, M. F. A New Facile Route to Flexible and Semi-Transparent Electrodes Based on Water Exfoliated Graphene and their Single-

Electrode Triboelectric Nanogenerator. *Adv. Mater.* **2018**, *30*, 1802953.
(26) De Sanctis, A.; Jones, G. F.; Townsend, N. J.; Craciun, M. F.; Russo, S. An Integrated and Multi-Purpose Microscope for the Characterization of Atomically Thin Optoelectronic Devices. *Rev. Sci. Instr.* **2017**, *88*, No. 055102.
(27) Zhu, S. E.; Yuan, S.; Janssen, G. C. A. M. Optical Transmittance of Multilayer Graphene. *EPL* **2014**, *108*, 17007.
(28) Ferrari, A. C.; Meyer, J. C.; Scardaci, V.; Casiraghi, C.; Lazzeri, M.; Mauri, F.; Piscanec, S.; Jiang, D.; Novoselov, K. S.; Roth, S.; Geim, A. K. Raman Spectrum of Graphene and Graphene Layers. *Phys. Rev. Lett.* **2006**, *97*, 187401.
(29) Koh, Y. K.; Bae, M. H.; Cahill, D. G.; Pop, E. Reliably Counting Atomic Planes of Few-Layer Graphene (n > 4). *ACS Nano* **2011**, *5*, 269−274.
(30) Romijn, J.; Vollebregt, S.; Dolleman, R. J.; Singh, M.; van der Zant, H. S. J.; Steenenken, P. G.; Sarro, P. M. A Miniaturized Low Power Pirani Pressure Sensor Based on Suspended Graphene. *IEEE 13th Annual International Conference on Nano/Micro Engineered and Molecular Systems (NEMS)*; IEEE 2018, 11−14.
(31) Bae, J. J.; Choi, H.; Lee, Y. H.; Lim, S. C. Pressure-Dependent Heat Transfer at Multilayer Graphene and Gas Interface. *Curr. Appl. Phys.* **2016**, 1236−1241.
(32) Kumar, S.; Bhatt, K.; Kumar, P.; Sharma, S.; Kumar, A.; Tripathi, C. C. Laser Patterned, High-Power Graphene Paper Resistor With Dual Temperature Coefficient of Resistance. *RSC Adv.* **2019**, 8262−8270.
(33) Kong, D.; Le, L. T.; Li, Y.; Zunino, J. L.; Lee, W. Temperature-Dependent Electrical Properties of Graphene Inkjet Printed on Flexible Materials. *Langmuir* **2012**, *28*, 13467−13472.
(34) di Bartolomeo, A.; Sarno, M.; Giubileo, F.; Altavilla, C.; Iemmo, L.; Piano, S.; Bobba, F.; Longobardi, M.; Scarfato, A.; Sannino, D.; Cucolo, A. M.; Ciambelli, P. Multiwalled Carbon Nanotube Films as Small-Sized Temperature Sensors. *J. Appl. Phys.* **2009**, *105*, No. 064518.
(35) Geim, A. K.; Novoselov, K. S. The Rise of Graphene. *Nat. Mater.* **2009**, *6*, 188−191.
(36) Shao, Q.; Liu, G.; Teweldebrhan, D.; Balandin, A. A. High-Temperature Quenching of Electrical Resistance in Graphene Interconnects. *Appl. Phys. Lett.* **2008**, *92*, 202108.
(37) Calizo, I.; Balandin, A. A.; Bao, W.; Miao, F.; Lau, C. N. Temperature Coefficients of the Raman Peaks for the Single-Layer and Bi-Layer Graphene. *Nano Lett.* **2007**, *7*, 2645−2649.


https://dx.doi.org/10.1021/acsami.0c08397
*ACS Appl. Mater. Interfaces* 2020, 12, 29861−29867